

Improved Near-infrared Luminescence of Si-rich SiO₂ with Buried Si Nanocrystals Grown by PECVD at Optimized N₂O Fluence

Chia-Yang Chen^a, Chun-Jung Lin^a, Hao-Chung Kuo^a, Gong-Ru Lin^{*a}, Yu-Lun Chueh^b, Li-Jen Chou^b, Chih-Wei Chang^c and Eric Wei-Guang Diau^c

^aDepartment of Photonics & Institute of Electro-Optical Engineering, National Chiao Tung University,
National Chiao Tung University
1001, Ta Hsueh Road, Hsinchu, Taiwan 300, R.O.C.

^bDepartment of Materials Science and Engineering, National Tsing Hua University,
101, Section 2 Kuang Fu Road, Hsinchu, Taiwan 300, R. O. C.

^cDepartment of Applied Chemistry, National Chiao Tung University,
1001, Ta Hsueh Road, Hsinchu, Taiwan 300, R. O. C.

ABSTRACT

The optimized N₂O fluence for plasma enhanced chemical vapor deposition (PECVD) growing silicon-rich substoichiometric silicon oxide (SiO_x) with buried Si nanocrystals is demonstrated. Strong room-temperature photoluminescence (PL) at 550-870 nm has been observed in SiO_x thin films grown by PECVD with N₂O fluence varying from 105 to 130 sccm. After annealing from 15 to 180 min, a 22-nm-redshift of the PL has been detected. The maximum PL intensity is observed for the 30-min annealed SiO_x growing at N₂O fluence at 120 sccm. Larger N₂O fluence and longer annealing time causes a PL blueshift by 65 nm and 20 nm, respectively. Such a blueshift is attributed to shrinkage in the size of the Si nanocrystals under the participation of dissolved oxygen atoms from N₂O. The (220)-oriented Si nanocrystals with radius ranging from 4.4 to 5.0 nm are determined. The luminescent lifetimes lengthens from 20 μs to 52 μs as the nc-Si size extends from 4.0 to 4.2 nm. Optimal annealing times for SiO_x preparing at different N₂O fluences and an optimum N₂O fluence of 120 sccm are reported. Serious oxidation effect at larger N₂O fluence condition is observed, providing smaller PL intensity at shorter wavelengths. In contrast, the larger size nc-Si will be precipitated when N₂O fluence becomes smaller, leading to a weaker PL at longer wavelength. These results provide the optimized growth condition for the Si-rich SiO₂ with buried Si nanocrystals.

Keywords: Si-rich SiO₂, photoluminescence, Nanocrystallite silicon, TEM, PECVD, TRPL

1. INTRODUCTION

Silicon nanocrystals (nc-Si) have been precipitated from the Si-rich silicon dioxide (SRSO) layer which is produced by several techniques such as high-dosage Si-ion-implantation in SiO₂^{1,2}, laser ablation³, electron-beam evaporation⁴, sputtering⁵ and plasma enhanced chemical vapor deposition (PECVD)⁶. It has been demonstrated that the photoluminescence (PL) from the nc-Si was enhanced with the increasing the annealing-temperature. Moreover, the peak wavelength slightly redshifts with the increasing temperature of the thermal treatment. Such results have been explained by quantum confinement theory⁶. The quantum-confined nc-Si enlarge the band gap and increase the spatial overlaps of the electron and hole wave functions in Si, thus increasing the spontaneous emission rate and shifting the emission peak to energies higher than the crystalline Si band gap⁷. Iacona *et al.*⁸ demonstrated that the PL wavelength is increasing from 770nm to 880 nm as the annealing temperature rises from 1100°C to 1300°C. They also demonstrated the change of λ_{max} (from 740 nm to 910 nm) at varied N₂O/SiH₄ flowing ratio (ranging between 6 and 15), which correlates to the increase in Si composition in SiO_x films between 33 and 44 at. %. The PL intensity of the 1200°C-annealed SiO_x sample with 42 at. % of Si content is highest. Oliveira *et al.*⁷ also observed that demonstrated by varying the N₂O/SiH₄ flow ratio between 0.25 and 0.5 and keeping SiH₄ flow of 15 sccm. After deposition, the films were thermally annealed in N₂ ambient, at temperatures from 450 to 1000°C for 2 h. The PL spectra for the as-deposited samples exhibit a broad emission band in 1.5-2.1 eV range. The contribution of two peaks can be distinguished at ~ 1.6 and 1.9 eV. After heat treatment, the PL of the samples grown with R = 0.3 and 0.5 were

*grlin@faculty.nctu.edu.tw; phone: 886-3-5712121 ext.56376; fax: 886-3-5716631

observed that the overall emission is more intense in the as-deposited films for all the samples studied. For the sample grown with $R = 0.3$, which has a higher Si content, both PL peaks decrease and shift towards lower energy after the annealing steps at 450 and 550°C. After the heat treatment at 750°C, the lower energy peak vanishes, the one at ~ 1.8 eV increases and a lower intensity peak around 2.1 eV appears. After the annealing at 1000°C, the PL intensity decreases and tends to energize higher than 2 eV.

Varying the N_2O/SiH_4 flow ratio is known to control the Si content, however, the correlation between N_2O/SiH_4 ratio and excess Si density as well as nanocrystallite Si size is not clear. In particular, the optimized annealing condition could also be changed for the SiO_x grown different N_2O/SiH_4 ratios. Since the control of SiH_4 fluence is unavailable to give a predictable result according to previous results, we investigate in this work the effect of N_2O fluence and annealing time on the PL intensity and wavelength. We also investigate the visible PL and time-resolved photoluminescence (TRPL) from PECVD SiO_x thin films after post-deposition annealing in N_2 ambient by varying the annealing times under the optimal N_2O fluence. The morphology of PECVD-grown SiO_x thin film was investigated using transmission electron microscope (TEM) to support the existence of nc-Si.

2. EXPERIMENT

The SiO_x films were grown on p-type Si (100) substrate by using PECVD system at pressure of 70 mTorr with different SiH_4 and N_2O fluences under forward power of 60 W. The N_2O fluence was varied from 105 sccm to 130 sccm. After deposition, the samples were annealed in a quartz furnace at 1100°C under N_2 flowing for 15 min to 180 min. The structure and optical properties of these films have studied by TEM, PL and time-resolved photoluminescence (TRPL). The room temperature PL of the SiO_x films were pumped by He-Cd laser at wavelength and average power intensity of 325 nm and 5 W/cm² and analyzed with a fluorescence spectrophotometer (Jobin Yvon, TRIAX-320 with resolution of 0.06 nm) and a cooled photomultiplier (Jobin Yvon, Model 1424M). In order to support the existence of nc-Si, the bright-field cross-section viewing photograph had taken by using TEM (JEOL 4000EX) operating at 400 keV with a point-to-point resolution of 0.18 nm. In the TRPL experiment, the samples were pumped by a YAG laser (NY 60, Countinous) at 355 nm (the repetition rate is 1 Hz, the pulse full width of half maximum (FWHM) is 60 ps, and average power is 0.5 mJ/pulse) and detected by a time-correlated single-photon counting system at wavelength corresponding to the PL of nc-Si ($\lambda = 760$ nm).

According to Einstein's two-level quantized radiation model⁴, the PL intensity of nc-Si can be approximated by $(I = \eta \sigma \phi(t) N / \tau)$, where σ is the absorption cross-section of nc-Si that can be calculated by a theoretical approach of $\sigma = \lambda^2 / 8\pi \Delta \nu \tau$ ^{10,11} (λ and $\Delta \nu$ are the peak wavelength and linewidth of the PL spectrum), η is a relative coefficient, τ is the lifetime of nc-Si, $\phi(t)$ is the pumping flux and N is the nc-Si concentration¹²⁻¹⁴. In the TRPL experiment, the correlation among the emission (absorption) cross-section, density and lifetime of nc-Si has to be obtained from the rate equation of a two-level system. The rate equation of the two-level system⁹ is

$$-\frac{dN_1}{dt} = \frac{dN_2}{dt} = -A_{21}N_2 + B_{12}N_1\rho(\nu) - B_{21}N_2\rho(\nu) \quad (1)$$

where N_1 and N_2 are the population density in the state 1 and state 2, A_{21} is the spontaneous emission coefficient, B_{21} is the stimulated emission coefficient and $\rho(\nu)$ is the radiation density per frequency interval.

Since there is no stimulated emission in the TRPL analysis, the rate equation is simplified as

$$-\frac{dN_1}{dt} = \frac{dN_2}{dt} = -A_{21}N_2 + B_{12}N_1\rho(\nu) \quad (2)$$

Assuming that N_1 equals to nc-Si and A_{21} equals to a reciprocal lifetime, in the steady state, the electron density in the state 2 (N_2),

$$N_2 = \frac{B_{12}}{A_{21}}N_1\rho(\nu) = B_{12}\tau_{nc-Si}\rho(\nu)N_{nc-Si} \quad (3)$$

$$B_{21} = \frac{c^3 A_{21}}{8 \pi n^2 n_g h \nu^3}$$

According to the Einstein relations of $B_{21}=B_{12}$ and

$$N_2 = \frac{c^3 A_{21}}{8\pi n^2 n_g h\nu^3} \rho(\nu) \tau_{nc-Si} N_{nc-Si} = \frac{\int I_{PL} dt A}{h\nu}, \quad (4)$$

By expressing $\rho(\nu) = \int \phi(t) dt A$ (A is the spot size of the pumping laser), we have

$$\int I_{PL} dt = \frac{c^3 A_{21}}{8\pi n^2 n_g h\nu^3} \frac{h\nu}{A} \int \phi(t) dt A \tau_{nc-Si} N_{nc-Si}, \quad (5)$$

Assuming a rectangular PL function of I_{PL} and a rectangular pump function of $\phi(t)$, we can rewrite Eq. (5) as

$$I_{PL} \tau_{PL} \cong \frac{c^3}{8\pi n^2 n_g \nu^2} \phi(t) N_{nc-Si} \tau_{pump}, \quad (6)$$

$$I_{PL} = \eta' \sigma N_{nc-Si} \phi(t) \frac{\tau_{pump}}{\tau_{PL}} \propto \sigma \phi(t) \tau_{PL}^{-1} N_{nc-Si}, \quad (7)$$

The theoretically equation (7) is also obtained in other papers¹⁴⁻¹⁶, as expressed by $I \propto \sigma \phi(t) \frac{\tau}{\tau_R} N$, for estimating the variations of nc-Si density through the PL intensity and lifetime.

3. RESULTS AND DISCUSSION

The PL spectra of PECVD-grown SiO_x films under 120-sccm N_2O -fluence as a function of annealing time were shown in Fig. 1. It was found that there is a broadened PL spectrum between 400 nm and 650 nm, which is attributed to the radiative defects including neutral oxygen vacancy (NOV)¹⁷ and the non-bridging oxygen hole center (NBOHC)¹⁸ in the as-grown SiO_x sample.

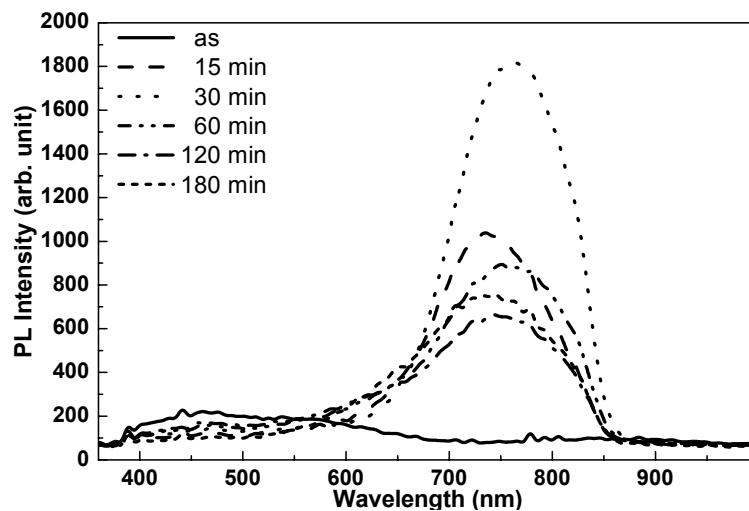


Fig. 1. Annealing-time dependent of PL intensities under the N_2O fluence at 120 sccm.

After annealing at 1100°C for 15 min, the defect-related PL is eliminated and the PL at 735 nm was enhanced. The central wavelengths and their FWHM of PL spectra for samples annealing from 15 min to 180 min were changed from 735 nm to 761 nm and 132.5 nm to 177 nm, respectively. In particular, the strongest PL appears in the 30-min annealed sample. The red shift in PL for the 30-min annealed sample was about 26 nm; however, a blue-shift phenomenon is observed after longer annealing time. In a 180-min annealed sample, the blue shift is up to 16.5 nm. Previously, Iacona *et al.*⁸ also found the strong PL in the wavelength ranging from 650 nm to 950 nm, which is attributed to the nc-Si clusters in high-temperature annealed PECVD-grown SiO_x film.

The nc-Si diameter as a function of annealing time by the rule of $\lambda = 1.24 / (1.12 + 3.73 / d^{1.39})^7$ was shown in Fig. 2. From the above equation, the size of nc-Si is proportional directly to the central wavelength of PL spectra. It shows that the thermal annealing process helps the formation and the size increasing of nc-Si during the first annealing process, so the red shift in PL was shown. This leads to the increasing quantity and wavelength of nc-Si with lengthening annealing time during the first 30 min. Later on, the oxygen atoms bond with the silicon atoms of nc-Si, which not only cause the reduction in nc-Si size, but also decrease the nc-Si density. As a result, the PL wavelength blue shifts, its FWHM enlarges and the PL intensity becomes weaker slowly.

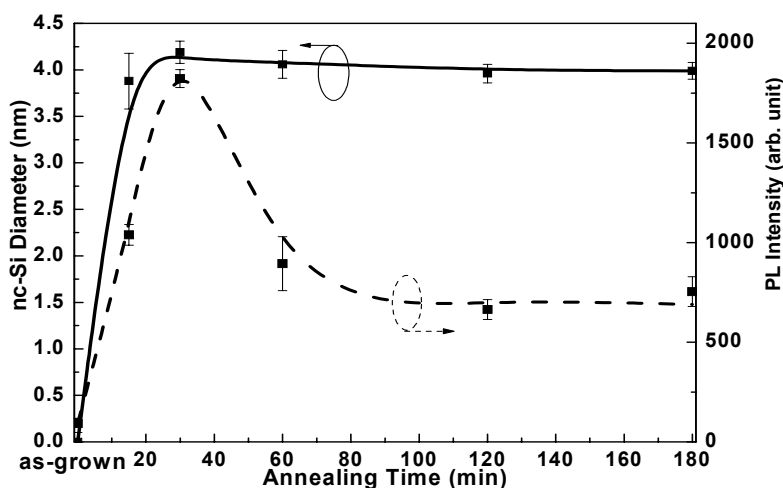


Fig. 2. PL intensity and size of the nc-Si in SiO_x film under different annealing times.

In the inchoative experiment, the SiO_x samples were manufactured by changing one of the SiH_4 and N_2O fluences. However, the PL spectrum was unavailable to give a predictable result for samples with varying SiH_4 fluences. Therefore, the SiO_x samples were prepared by changing N_2O fluences from 105 sccm to 130 sccm, and the thick were in the range from 195 nm to 258 nm. The SiO_x samples were annealed at 1100°C for 30 min to obtain a maximum PL intensity, as shown in figure 3. As the N_2O fluence increased from 105 sccm to 120 sccm, the PL intensity at 120 sccm is enhanced 4 times larger than that at 105 sccm, but the PL intensity is decreased 3 times while the N_2O fluence increased to 130 sccm. The central PL wavelength decreases to 606.5-624.5 nm when the N_2O fluence is higher or lower than the optimum fluence. As the N_2O fluence detunes larger than the optimized N_2O fluence, the oxidation of excess silicon atoms become significant, which degrade the nc-Si related PL signal. Both the size and PL intensity of nc-Si become smaller in this case. In contrast, more excess Si atoms will exhibit in the SiO_x film as the N_2O fluence less than the optimal one, which leads to an increasing size of the buried nc-Si, and the larger size of nc-Si causes a smaller density as well as a smaller PL intensity. Nonetheless, the PL wavelength of the N_2O fluence less than the optimal one was not larger than the N_2O fluence more than the optimal one. It shows the correlative size of nc-Si was smaller than the latter one (the N_2O fluence more than 120 sccm).

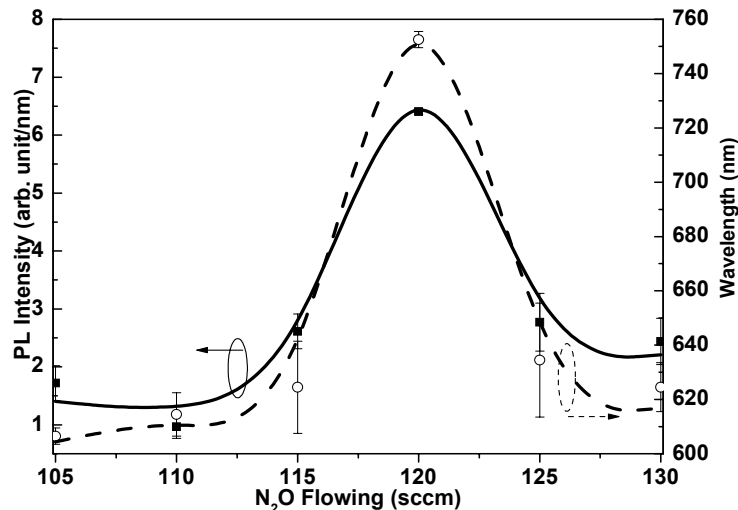


Fig. 3. PL intensity and wavelength of nc-Si in SiO_x film under different values of N₂O fluence after 30 min annealing.

In Fig. 1, it is evident that a sufficient annealing time to precipitate the nc-Si with suitable size and maximum density. Note that the annealing time may be varied for samples growing with different N₂O fluence. This is the reason between the variance of the correlative sizes as the N₂O fluences less or more than 120 sccm. The optimized annealing times of samples preparing under different N₂O fluences were shown in Fig. 4.

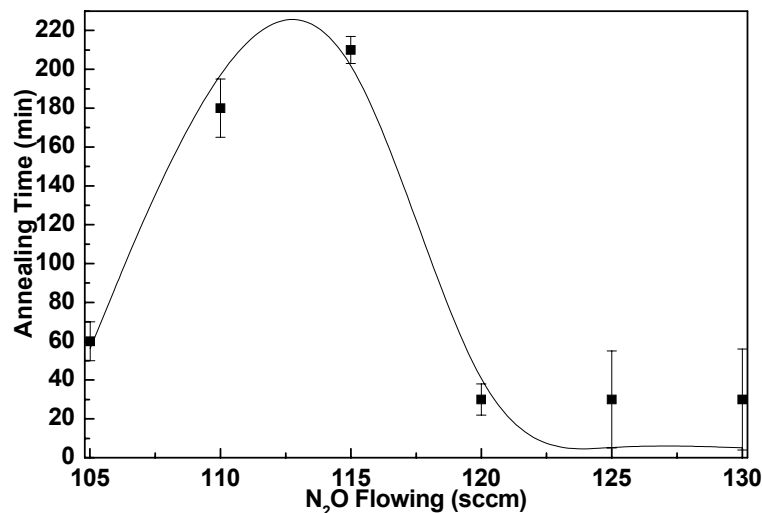


Fig. 4. Optimal annealing time of the SiO_x film under different values of N₂O fluence.

The annealing time become longer (60-210 min) for smaller N₂O-fluence conditions, whereas it is shorter than 30 min for the N₂O fluence >120 sccm. The PL intensity and wavelength of all samples at the optimal annealing time under different N₂O fluences are shown in Fig. 5. The PL wavelength first decreases from 733 nm to 754.5 nm as the N₂O fluence increases from 105 sccm to 120 sccm, and then decreases to 690 nm at N₂O fluence of 130 sccm or larger. The size of nc-Si becomes larger as the N₂O fluence is smaller than optimum value (120 sccm), which is attributed to the more excess Si under less N₂O fluence. The evolutions of PL intensity and wavelength under different N₂O fluences in Fig. 5 were correlated to the above discussion.

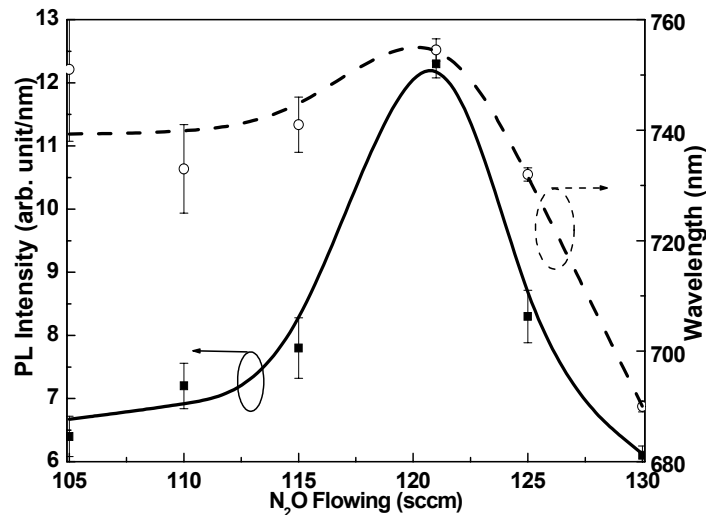


Fig. 5. PL intensity and wavelength of nc-Si in SiO_x film under different N₂O fluence at optimal annealing times.

The bright-field cross-section viewing photograph of TEM analysis for the optimized sample (the N₂O fluence at 120 sccm and 30-min 1100°C annealing) is shown in Fig. 6, which supports the existence of nc-Si. The lattice distance between two (111)-oriented planes of 0.63 nm observed from a Si substrate is employed as a standard ruler in this picture, which helps to estimate the smaller plane-to-plane distance of nc-Si of about 0.19 nm. According to the X-ray diffraction (XRD) data, the oriented planes of nc-Si structure are determined as (220), which is in good agreement with the reference data. The sizes of nc-Si are distributed from 4.4 nm to 5 nm from the TEM analysis.

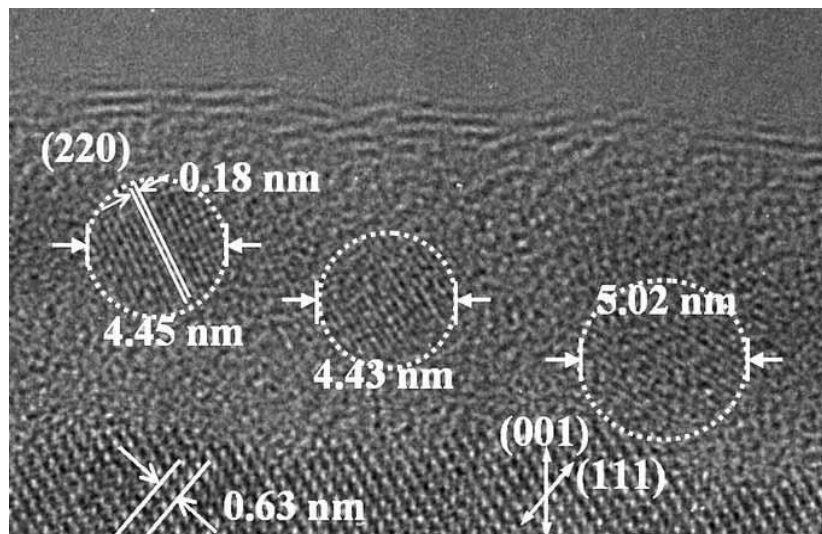


Fig. 6. The TEM micrograph of the cross section of the SiO_x film annealed at 1100°C for 30 min.

The TRPL results of SiO_x samples at 1100°C for different annealing time are shown as Fig. 7 and in the Table 1. A stretched exponential function: $I(t) = I_0 \exp(-t/\tau)$ was used to fit the data, in which τ is an effective decay time of nc-Si. The luminescent lifetime lengthens from 20 to 52 μ s as the nc-Si size extends from 4.0 to 4.2 nm; the nc-Si lifetime increases smoothly with the increment of nc-Si size, which has the same temper by Garcia *et al.*¹⁵.

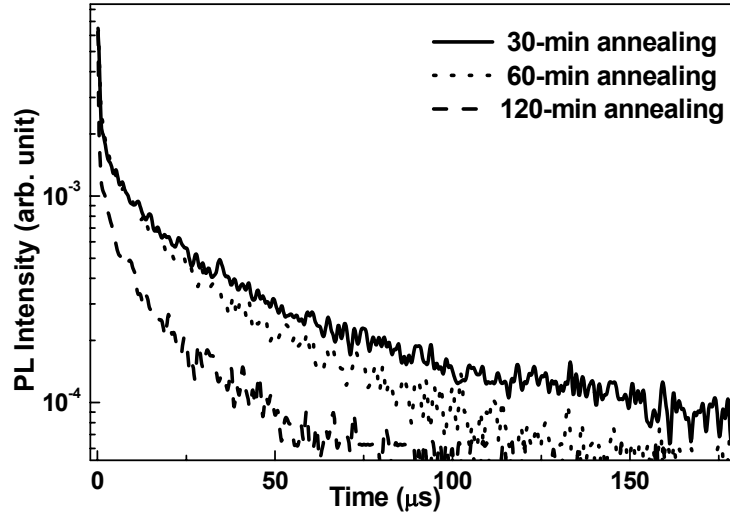


Fig. 7. TRPL of nc-Si in SiO_x films at different annealing times.

The theoretical carrier-transition equation can be simplified as $I_{PL} \propto \sigma\phi(t) \frac{1}{\tau_{PL}} N_{nc-Si}^{15,19}$, and the variation of the nc-Si density can be estimated by the PL intensity (I_{PL}) and lifetime (τ_{PL}) of nc-Si, where σ and $\phi(t)$ are the emission (absorption) cross-section of nc-Si and the pumping photon flux density obtained from the pumping power, respectively, and their multiplication for different annealing-time samples are a constant. As the annealing time lengthens from 30 to 120 min, the density of nc-Si is decreased from $8.3 \times 10^{22} \text{ cm}^{-3}$ to $1.2 \times 10^{22} \text{ cm}^{-3}$, which are correlated with the evolution of measured PL and the results also reported by Augustine *et al.*¹⁹.

4. CONCLUSIONS

The optimized N₂O fluence for PECVD-grown SiO_x films with buried nc-Si is demonstrated. Strong PL at 550-870 nm that attributed to nc-Si has been observed in SiO_x thin films with N₂O fluence varying from 105 to 130 sccm. After annealing from 15 to 180 min, a 22-nm-redshift of the PL has been detected. The maximum PL intensity at 761 nm emitting is observed for the 30-min annealed SiO_x growing at 120-sccm N₂O-fluence. Larger N₂O fluence and longer annealing time cause a PL blueshift by 65 nm and 20 nm, respectively. Such a blueshift is attributed to shrinkage in the size of the nc-Si under the participation of dissolved oxygen atoms from N₂O. We demonstrated that nc-Si need some time to grow up, and then have the maximum PL intensity and size of nc-Si, finally continuative decreased due to the participant of the O atoms from N₂O fluence. It means the nc-Si needs the different optimal annealing time to add up the maximum PL intensity under different N₂O fluences, i.e. different recipe has different annealing time even at the same annealing temperature. The (220)-oriented nc-Si with diameter ranging from 4.4 to 5.0 nm is determined. The luminescent lifetime lengthens from 20 μs to 52 μs as nc-Si size extends from 4.0 to 4.2 nm and the correlated density decreased from $8.3 \times 10^{22} \text{ cm}^{-3}$ to $1.2 \times 10^{22} \text{ cm}^{-3}$.

Table 1. The wavelength, size, lifetime and estimated density of nc-Si after annealing for 30, 60 and 120 min.

		30 min	60 min	120 min
Wavelength	(nm)	761	751	743
nc-Si Size	(nm)	4.2	4.1	4.0
Lifetime	(μs)	52	31	20
Estimated Density	(cm ⁻³)	8.3×10^{22}	2.4×10^{22}	1.2×10^{22}

ACKNOWLEDGEMENT

The authors would like to thank the National Science Council of the Republic of China, Taiwan for partially supporting this research under Contract No. NSC92-2215-E-009-028 and NSC93-2215-E-009-007.

REFERENCES

1. T. Shimizu-Iwayama, K. Fujita, S. Nakao, K. Saitoh, T. Fujita, and N. Itoh, "Visible photoluminescence in Si⁺-implanted silica glass", *J. Appl. Phys.* **75**, pp. 7779-7783, 1994.
2. K. S. Min, K. V. Shcheglov, C. M. Yang, H. A. Atwater, M. L. Brongersma, and A. Polman, "Defect-related versus excitonic visible light emission from ion beam synthesized Si nanocrystals in SiO₂", *Appl. Phys. Lett.* **69**, pp. 2033-2035, 1996.
3. E. Werwa, A. A. Seraphin, L. A. Chin, Chuxin Zhou, and K. D. Kolenbrander, "Synthesis and processing of silicon nanocrystallites using a pulsed laser ablation supersonic expansion method", *Appl. Phys. Lett.* **64**, pp. 1821-1823, 1994.
4. H. Morisaki, F. W. Ping, H. Ono, and K. Yazawa, "Above-band-gap photoluminescence from Si fine particles with oxide shell", *J. Appl. Phys.* **70**, pp. 1869-1870, 1991.
5. S. Hayashi, T. Nagareda, Y. Kanzawa, and K. Yamamoto, "Photoluminescence of Si-Rich SiO₂ Films: Si Clusters as Luminescent Centers", *Jpn. J. Appl. Phys. Part 1* **32**, pp. 3840-3845, 1993.
6. F. Z. Song, and X. M. Bao, "Visible photoluminescence from silicon-ion-implanted SiO₂ film and its multiple mechanisms", *Phys. Rev. B* **55**, pp. 6988-6993, 1997.
7. C. Delerue, G. Allan, and M. Lannoo, "Theoretical aspects of the luminescence of porous silicon", *Phys. Rev. B* **48**, pp. 11024-11036, 1993.
8. F. Iacona, G. Franzò, and C. Spinella, "Correlation between luminescence and structural properties of Si nanocrystals", *J. Appl. Phys.* **87**, pp. 1295-1303, 2000.
9. J. T. Verdeyen, *Laser Electronics*, pp 179-182, Englewood Cliffs, NJ:Prentice Hall, 1995.
10. O. Madelung, *Introduction to Solid State Theory*, Ch. 6, Berlin:Springer-Verlag, 1978.
11. S. Donati, *Photodetectors Devices, Circuits, and Applications*, p. 11, Upper Saddle River, NJ:Prentice Hall, 2000.
12. D. Pacifici, E. C. Moreira, G. Franzò, V. Martorino, F. Priolo, and F. Iacona, "Defect production and annealing in ion-irradiated Si nanocrystals", *Phys. Rev. B* **65**, p. 144109, 2002.
13. F. Priolo, G. Franzò, D. Pacifici, V. Vinciguerra, F. Iacona, and A. Irrera, "Role of the energy transfer in the optical properties of undoped and Er-doped interacting Si nanocrystals", *J. Appl. Phys.* **89**, pp. 264-272, 2001.
14. D. Kovalev, J. Diener, H. Heckler, G. Polisski, N. Kunzner, and F. Koch, "Optical absorption cross sections of Si nanocrystals", *Phys. Rev. B* **61**, pp. 4485-4487, 2000.
15. C. Garcia, B. Garrido, P. Pellegrino, R. Ferre, J. A. Moreno, J. R. Morante, L. Pavesi, and M. Cazzanelli, "Size dependence of lifetime and absorption cross section of Si nanocrystals embedded in SiO₂", *Appl. Phys. Lett.* **82**, pp. 1595-1197, 2003.
16. M. Lopez, B. Garrido, C. Garcia, P. Pellegrino, A. Perez-Rodriguez, J. R. Morante, C. Bonafos, M. Carrada, and A. Claverie, "Elucidation of the surface passivation role on the photoluminescence emission yield of silicon nanocrystals embedded in SiO₂", *Appl. Phys. Lett.* **80**, pp. 1637-1639, 2002.
17. H. S. Bae, T. G. Kim, C. N. Whang, S. Im, J. S. Yun, and J. H. Song, "Electroluminescence mechanism in SiO_x layers containing radiative centers", *J. Appl. Phys.* **91**, pp. 4078-4081, 2002.
18. H. Nishikawa, T. Shiroyama, R. Nakamura, Y. Ohki, K. Nagasawa, and Y. Hama, "Photoluminescence from defect centers in high-purity silica glasses observed under 7.9-eV excitation", *Phys. Rev. B* **45**, pp. 586-591, 1992.
19. B. H. Augustine, E. A. Irene, Y. J. He, K. J. Price, L. E. McNeil, K. N. Christensen, and D. M. Maher, "Visible light emission from thin films containing Si, O, N, and H", *J. Appl. Phys.* **78**, pp. 4020-4030, 2000.